RSC Advances



This is an *Accepted Manuscript*, which has been through the Royal Society of Chemistry peer review process and has been accepted for publication.

Accepted Manuscripts are published online shortly after acceptance, before technical editing, formatting and proof reading. Using this free service, authors can make their results available to the community, in citable form, before we publish the edited article. This Accepted Manuscript will be replaced by the edited, formatted and paginated article as soon as this is available.

You can find more information about *Accepted Manuscripts* in the **Information for Authors**.

Please note that technical editing may introduce minor changes to the text and/or graphics, which may alter content. The journal's standard <u>Terms & Conditions</u> and the <u>Ethical guidelines</u> still apply. In no event shall the Royal Society of Chemistry be held responsible for any errors or omissions in this *Accepted Manuscript* or any consequences arising from the use of any information it contains.



Core-shell nanospherical polypyrrole/graphene oxide composites for high performance supercapacitors

Wenling Wu^a, Liuqing Yang^b, Suli Chen^a, Yanming Shao^a, Lingyun Jing^a, Guanghui Zhao^{a*} and Hua Wei^{a*}

^aState Key Laboratory of Applied Organic Chemistry, Key Laboratory of Nonferrous Metal Chemistry and Resources Utilization of Gansu Province, College of Chemistry and Chemical Engineering, Lanzhou

University, Lanzhou 730000, PR China

Abstract

The novel core-shell polypyrrole/graphene oxide (PPy-GO) nanomaterials of uniform PPy nanospheres and GO have been synthesized by *in situ* surface-initiated polymerization method. The morphology and structure of the core-shell PPy-GO composites were studied by means of techniques. Experimental results showed that PPy nanospheres with small nanospheres of only ~70 nm were uniformly grown on the GO sheets to form continuous 3D core-shell PPy-GO nanocomposite. The smaller size of PPy can not only be more beneficial to increasing the electrochemical performance, but can also reduce ion diffusion path and make higher material utilization. Moreover, the well-designed core-shell nanostructure and synergistic effects of PPy-GO composites can clearly lead to high rates of electrode reaction and good electrode/electrolyte contact areas. Meanwhile, its electrochemical performance was evaluated by cyclic voltammetry (CV), galvanostatic charge/discharge (GCD) and electrochemical impedance spectroscopy (EIS) tests. The specific capacitance of core-shell PPy-GO nanocomposite can reach up to 370 F/g at a current density of 0.5 A/g with a large mass loading of 8.0 mg/cm². It is noteworthy that the cycling stability of PPy-GO electrode

^b State Key Laboratory of Electrical Insulation and Power Equipment, School of Electrical Engineering,

Xi'an Jiaotong University, Xi'an, 710049, PR China

^{*} Corresponding author. E-mail address: zhaogh@lzu.edu.cn (G. H. Zhao)

^{*} Corresponding author. E-mail address: weih@lzu.edu.cn (H. Wei)

was improved significantly by the core-shell nanostructures, and showed excellent capacitance retention (91.2%) even after 4000 cycles, suggesting its attractive application in supercapacitors with improved performance.

Keywords: supercapacitors; polypyrrole; graphene oxide; core-shell; nanocomposites.

1. Introduction

With the critical issue of environmental pollution, the increasing demand for sustainable and renewable energy storage systems applied in hybrid vehicles and portable electronic devices requires the development of novel materials with superior electrochemical performances.[1] Among the various systems that lead the state-of-the-art electrical energy storage systems, supercapacitors, are considered as one of the promising candidates due to low-cost, environmental-friendly, fast charging/discharging rate, sustainable cycle stability, high power density and excellent cycling life.[2,3] According to their charge storage mechanism, supercapacitors are divided into electrochemical double layer capacitors (EDLCs) and pseudosupercapacitors. [4,5] EDLCs store energy by rapid electrostatic charge accumulation at the interface between electrolyte and electrode, and these high specific area active materials, such as carbon materials, [6,7] which have high power density and long cycle life but relatively low specific capacitance because of the limited electrochemically available surface area.[8] By comparison, pseudosupercapacitors, such as conducting polymers (CPs)[9-11] and transition metal oxides[12,13], store energy through a reversible redox or Faradic charge transfer reactions at the electrode surface, [1,14] which can increase the specific capacitance and extends the operation voltage of the supercapacitor,[8] but the power density and durability are relatively low.[15] Therefore, the development of novel materials for high performance supercapacitors demands the appropriate combination of pseudocapacitance and EDLCs, morphology, good electrochemical performance, good cycling stability, excellent capacitance retention and high mass loading, which is required for many practical applications.[16,17] Of the various CPs, Polypyrrole (PPy) is an advanced electrode material for supercapaciters because of their inherent fast redox switching, high energy-storage capacity, ease of synthesis in aqueous solution, good electrical conductivity, and stability in ambient air.[18,19] However, PPy sufferes from a limited stability during charge/discharge processes and reduce the initial performance, which result in mechanical degradation of the electrodes, restricting of the practical applications. [20] To date, Many efforts have been made to improve electrochemical performance of PPy by the development of promising graphene or GO. As we all know, graphene or GO has been extensively researched and exhibit excellent characteristics in many applications due to its good electrical conductivity, high mechanical strength, and excellent chemical stability.[21] Meanwhile, the results indicated that the PPy-GO nanocomposites can not only enhance the mechanical and electrochemical properties of composites but also the composites regulate the properties of individual component with a synergistic effect.[22] Furthermore, it is noteworthy that it is challenging to achieve excellent electrochemical performance, cyclic stability and favourable capacitance retention for PPy-GO electrodes with high mass loadings, which is very important for many practical applications. For example, zhang et al. reported that polypyrrole/graphene hydrogel (PPy/GH) composites could achieve the specific capacitance of 375 F/g at a scan rate of 10 mV/s and the capacitance retention of 87% after 4000 cycles, but the mass loading was only ~1.0 mg/cm².[23] Zhu et al. demonstrated that electrodeposition of GO/PPy nanocomposites could obtain the specific capacitance of 356 F/g at a current density of 0.5 A/g and the capacitance retention of 78% after 1000 cycles.[24] Fan et al. exhibited that the GO/PPy composites could gain the specific capacitance of 332.6 F/g at a current density of 0.25 A/g and 89.6% of the capacitance retention after 4000 cycles, but the mass loading was only 5.2 mg/cm².[25] From the above reports, it can also be concluded that the specific capacitance and the capacitance retention will be decreased with the increase of mass loading due to the increased self-aggregation, difficulty of charge transfer and electrolyte permeation. Therefore, the electrodes materials with high mass loading having good special capacitance and excellent cycling stability give desired candidate for scalability as it is close to the realistic mass content of commercial devices.[26]

Based on the above considerations, we have fabricated the 3D core-shell nanosphereical PPy-GO composites by *in situ* surface-initiated polymerization of pyrrole (Py) in the presence of GO and used an electrode material for supercapacitors. PPy nanospheres were uniformly grown on the GO sheets. Our results indicated that the core-shell nanosphereical PPy-GO electrodes demonstrated high specific capacitance, good cycling stability and excellent capacitance retention with high mass loading, which was ascribed to the relatively small size of PPy nanospheres and the synergistic effect between the GO and PPy of core-shell PPy-GO composites. Moreover, this facile method for the synthesis of PPy-GO nanocomposites should be very promising for the fabrication of inexpensive, good-performance electrochemical supercapacitors.

2. Experimental

2.1 Materials

Pyrrole monomer (Py) dehydrated with calcium hydride for 24 h was distilled under reduced pressure before use. Ammonium persulfate (APS), Polyvinyl Alcohol (PVA1788) and *p*-Toluenesulfonic acid (*p*-TSA) were purchased from the Tianjin Chemical Reagent Co. All others chemical reagents were analytical grade and used without further purification. The double-distilled water was used throughout.

2.2 Preparation of GO-PPy nanostructures

GO was synthesized using a modified Hummer's method and dispersed in water with the concentration of 3.5 mg/mL by ultrasonication for 3 h; the details of the procedure developed by our group were described elsewhere.[27] The polymerization way of GO-PPy

nanocomposites were as follows (Table 1): 65 mL distilled water was added in a round-bottom flask with 0.1 g PVA and 0.1 g *p*-TSA and stirred for 0.5 h at room temperature. Then 0.5 mL of Py and GO (3.5 mg/mL, 15 mL) were added and vigorously stirred for 0.5 h. Next, 20 mL of 1.14 g (0.005 mol) aqueous solution of APS was added drop by drop into the reaction mixture, and kept stirring in the ice-bath for 12 h. The dark product was washed three times with deionized water and ethanol. Finally, the product was dried in a vacuum oven at 60 °C for 24 h to obtain a dark powder.

Meanwhile, PPy (S0) was also fabricated without GO component under the same conditions.

(Table 1 in here)

2.3 Characterization methods

The morphology and structure of PPy and GO-PPy nanocomposites were examined by an S-4800 field-emission scanning electron microscope (FE-SEM, HITACHI, Tokyo, Japan) and a JEM-1200 EX/S transmission electron microscope (TEM, JEOL, Tokyo, Japan). The as-prepared samples were measured on Fourier transform infrared (FTIR, Impact 400, Nicolet, Waltham, MA) spectroscopy and X-ray diffraction (XRD, Rigaku D/MAX-2400) with Cu K α radiation λ =0.154 nm. Raman spectra were determined by a Renishaw Microscope (RM-2000) with 532 nm wavelength incident laser light. Thermal gravimetric analysis (TGA, TA Instruments 2050) was analyzed under N₂ atmosphere with a heating rate of 10 °C/min from 35 to 800 °C.

2.4 Electrochemical measurements

Electrochemical measurements (CHI 660E, Chenghua, Shanghai, China) were carried out on a typical three-electrode cell setup at room temperature, in which stainless steel mesh loaded with electroactive material was used as the working electrode, standard calomel reference electrode (SCE) as the reference electrode, platinum plate $(1 \times 1 \text{ cm}^2)$ as the counter electrode, and $1.0 \text{ M H}_2\text{SO}_4$ solution as the electrolyte. The working electrode was fabricated by mixing

80 wt% of electroactive materials, 15 wt% of acetylene black and 5 wt% polytetrafluoroethylene (PTFE) suspension binder in ethanol to obtain homogeneous slurry. Then the slurry was coated on the stainless steel substrates (surface area 1×1 cm²) and allowed to be placed into a vacuum oven and was dried at 60 °C for 24 h. The mass loading of the electroactive material is 8 mg/cm².

Cyclic voltammetry (CV), galvanostatic charge-discharge (GCD) techniques and electrochemical impedance spectroscopy (EIS) experiments were performed with CHI660E electrochemical workstation at room temperature. CV measurements were taken from -0.2 to 0.8 V at different scan rates (10, 20, 40, 60, 80 and 100 mV s⁻¹) and GCD curves was carried out in the potential range of from -0.2 to 0.8 V with an applied current density of 0.5, 1.0 and 2.0 A/g. The specific capacitance (*Cs*) was calculated from the GCD curves according to the following equation:

$$Cs = \frac{I\Delta t}{\Delta Vm} \tag{1}$$

Where Cs is the specific capacitance (F/g), I is the charge-discharge current (A), Δt is the discharge time (s), ΔV represents the potential drop during discharge, and m is the mass of active material (g). EIS measurement was carried out in the frequency range 10^5 to 10^{-2} Hz at open circuit potential with an ac perturbation of 5 mV. Measurement of cycle-life stability was carried out by CV at a scan rate of 100 mV s^{-1} .

3. Results and discussion

3.1 Morphological analyses

The well-defined core-shell nanospheres of PPy-GO were successfully fabricated via the facile *in situ* surface-initiated polymerization method. The SEM and TEM images of the PPy-GO and PPy nanospheres were shown. It could be found from Fig. 1 (a, b, c) that the PPy nanospheres were composed exclusively of a large amount of uniform nanospheres with an

average diameter of about 70 nm. Interestingly, the homogeneous PPy nanospheres were formed with polyvinyl alcohol (PVA) as a surfactant in the solution. As is well known, PVA is a water-soluble polymer and have abundant OH groups in their trimly arranged structure, which could form the hydrogen bond between OH groups of PVA and hydrogen atoms in pyrrole and further induce an ordered structure of polypyrrole. In addition, the surfactants are amphipathic and hydrophobic substance solubilized. Hence, when the hydrophobic monomer pyrrole was added to the aqueous solution with PVA, it would get into the hydrophobic cavity formed by surfactant and form a lot of hydrogen bonds between them. Meanwhile, PVA has a valid trend to composite ordered structure. Afterward, this structure was facilitated by the intermolecular interaction and hydrogen bonds between pyrrole and PVA, which might ultimately induce the homogeneous PPy nanospheres, as presented in Scheme 1. Otherwise, the core-shell morphology of the PPy-GO composites can be also clearly observed from Fig. 1(d, e, f). As seen, the surface morphology of GO sheets that are coated on the surface of PPy nanospheres shows a typically crumpled and wrinkled structure. Additionally, it is revealed that PPy nanospheres with small sizes were uniformly grown on the surfaces of GO sheets, and the average size of PPy-GO nanospheres was similar to that of PPy, which is smaller size than the reported scale of PPy-GO.[28] The smaller size may be more beneficia for the enhancement of the electrochemical performance as an electrode for supercapacitors due to their large surface areas. This is a reason for that the nanocomposites with small size can short diffusion path and provide high electroactive regions during the oxidation and reduction of PPy, which is advantageous in the effective access of the electrolyte to the electrode. [29] Moreover, little agglomerate of PPy is observed, which could be connected with the specific interactions between GO and PPy, that is, the typically mentioned π - π stacking, donor-acceptor interactions and hydrogen bonding force (O-H···N),[30] as presented in Scheme 2. Prevention of PPy nanospheres from aggregating with GO means the decrease of migration and diffusion length of the electrolytes ions during the charge-discharge process.

(Fig. 1 in here)

(Scheme 1 in here)

(Scheme 2 in here)

3.2 FTIR spectra

FTIR spectra were used to analyze the chemical composition of the core-shell nanospherecial composites as well as the interactions between PPy and GO. Fig. 2 presents the FTIR spectra of GO, PPy and PPy-GO composites. Three characteristic peaks of GO at 3420, 1733 and 1063 cm⁻¹, indicating the presence of hydroxyl, carbonyl and epoxy groups, respectively. The PPy-GO (S1) nanocomposites showed the absorbance peaks at 1546 and 1470 cm⁻¹, associated with the symmetric and antisymmetric stretching vibrations of the pyrrole rings.[25] The bands at 1302 and 1045 cm⁻¹ were assigned to the stretching vibrations of C-N and the deformation vibrations of C-H, respectively. And the strong bands at 1183 and 916 cm⁻¹ demonstrate that the PPv is doped. Meanwhile, the peaks at 972 and 790 cm⁻¹ indicate that the presence of polymerized pyrrole. It is worthy of note that the characteristic peak in the core-shell nanospherical PPv-GO composites (at 1546 cm⁻¹) shifted to low wavenumbers compared with those for the PPy (at 1550 cm⁻¹), respectively. This further supports the existence of strong interactions such as π - π stacking between GO and PPy backbone and hydrogen bonding caused by the residual oxygen functional groups on GO.[31] All these results confirmed that we synthesized successfully the core-shell nanospherical PPy-GO composites.

(Fig. 2 in here)

3.3 Raman spectra

The interactions between PPy and GO were further characterized by Raman spectra, which are shown in Fig. 3. The Raman spectrum of the PPy-GO exhibited two outstanding peaks at

1372 cm⁻¹ and 1574 cm⁻¹ that can be ascribed to the well documented D and G bands of GO, respectively. In the Raman spectrum, the D band derives from the κ -point phonons with A_{1g} symmetry, while the G band corresponds to the E_{2g} phonon of sp² C atoms.[29] Additionally, the peaks at 968 and 1054 cm⁻¹ arise from the doped PPy structure. Furthermore, the intensity ratio (I_D/I_G) was 0.52, 0.61, 0.65, 0.66, 0.69 and 0.87 for the S0, S1, S2, S3, S4 and GO, respectively. With the increase of the content of GO, the intensity ratio (I_D/I_G) were enhanced, which indicated the introduction of GO sheets into PPy matrices. Compared with the PPy nanospheres, the core-shell PPy-GO nanocomposites demonstrated tiny shift in Raman peaks due to the π - π interaction of PPy chains with the GO sheets.[32] The representative Raman spectra results identify with those educt from the FTIR spectra.

(Fig. 3 in here)

3.4 XRD analysis

Fig. 4 illustrated the X-ray scattering patterns of the PPy and PPy-GO composites. As one can see, a broad reflection peak of the PPy from $2\theta = 20\text{-}30^{\circ}$ and an amorphous structure is observed.[33] The core-shell nanospherical PPy-GO composites exhibited broad scattering peak which are similar to those obtained from the pure PPy, meaning that no additional crystalline order has been introduced into the nanospherical composites. Additionally, the peak ascribed to GO within the composites disappeared,[34] demonstrating that the GO sheets is completely interacted with PPy molecules with the π -stacking and the electrostatic interactions.

(Fig. 4 in here)

3.5 Thermogravimetric analysis

The thermal stability is one of the important parameters for polymer materials. Therefore, the TG analysis of the PPy and the PPy-GO composites are shown in Fig. 5. The initial weight losses related to the PPy and PPy-GO composites at about 100 °C could be attributed to the

evaporation of surface absorbed water molecules of the samples. After that, major weight loss of PPy and PPy-GO composites takes place because of the degradation of the PPy backbones.[35] Meanwhile, the PPy presents 54% mass loss from 100 to 800 °C. The weight loss values of PPy-GO composites are found to be 37% between 100 and 800 °C. Obviously, it is also found that the PPy-GO composites demonstrate better thermostability than the PPy, which might result from the strong bonds interaction between PPy with the GO sheets.

(Fig. 5 in here)

3.6 Electrochemical studies

3.6.1 Cyclic voltammetry

To assess the electrochemical performance of core-shell PPy-GO nanocomposites as active materials for supercapacitor electrodes, it can be seen that CV recorded for the sample of active material in 1.0 M H₂SO₄ electrolyte in the potential range from -0.2 to 0.8 V. As can be seen in Figure 6, all CV curves are close to rectangular shape, implying that all samples have an ideal capacitive characteristics with ion response [36] Compared with PPy nanospheres (Fig. 6a), the core-shell nanospherical PPy-GO composite exhibits the larger current density responses at the same scan rate (100 mV/s), demonstrating its better capacitive performance. The high electrochemical performance of core-shell nanospherical PPy-GO composite may be ascribed to the well-designed core-shell nanostructure and synergistic effects between PPy and GO. Firstly, GO can clearly lead to high rates of electrode reaction and high electrode/electrolyte contact areas, resulting in enhanced electrochemical performance.[37] Secondly, PPy can greatly increase the pseudocapacitance contribution to the overall capacitance. [38] Next, the electrostatic interactions, π - π stacking and hydrogen-bonding interactions between GO sheet and PPy chains are also beneficial for enhancing the electrochemical performance.[30] Fig. 6b shows the CV curves of the core-shell nanospherical PPy-GO composite at different scan rates. It is noted that the peaks current density of PPy-GO increases remarkably with increasing potential scan rate from 10 to 100 mV/s, indicating its good rate capability and excellent capacitance behavior.

(Fig. 6 in here)

3.6.2 Galvanostatic charge/discharge

In order to assess the rate capability of the electrode material, the GCD curves at current densities were tested in 1.0 M H₂SO₄ solution and shown in Fig. 7. All curves present linear correlation between charge/discharge time and voltage, typical of a capacitor. It is found that the specific capacitance of the core-shell nanospherical PPy-GO composite was 370 F/g whereas for nanospheres of PPy it was 216 F/g at current density of 0.5 A/g. The PPy-GO electrode presented a high capacitance with high mass loading (8 mg/cm²) that may be mainly attribute to smaller particle sizes of PPy nanospheres and the well-defined core-shell nanostructures, which reduce the ion diffusion length and increase the kinetics of ion and electron transport in electrodes and at the electrode/electrolyte interface.[39] Additionally, the specific capacitance of PPy-GO was 370-144 F/g at current density ranging from 0.5 to 2.0 A/g (Fig. 7b). The specific capacitances for electrodes the PPy-GO and PPy were summarized in Table 1. Obviously, with the increase of discharge current densities, the capacitance of the core-shell nanospherical PPy-GO composite was decreased, which was likely derived from the internal resistance of electrode and the deficient Faradaic redox reaction of the active material under upper discharge current densities. At the same time, all the curves displayed the IR drop at the beginning of the discharging phase due to internal resistance, however, this was decreased at the lower current density of 0.5 A/g, which may be ascribed to the slow electrochemical process in which the electrolyte ions approach the deep pores.

Table 2 The specific capacitance of the core-shell nanospherical PPy-GO composite and PPy nanospheres at different current densities in an aqueous 1.0 M H₂SO₄ electrolyte.

Samples	Specific capacitance (F/g)

	0.5 A/g	1.0 A/g	2.0 A/g
PPy-GO	370	233	144
PPy	216	143	68

(Table 2 in here)

(Fig. 7 in here)

3.6.3 Cycling performance

The stability and reversibility of an electrode material are very key factors in determining supercapacitor electrodes for effective applications. PPy usually sustains a poor long-term stability during cycling because the shrinking and swelling of PPy may lead to degradation.[40] The cycling stability performance of the core-shell nanospherical PPy-GO composites and PPy nanospheres were tested at a scan rate of 100 mV s⁻¹ for 4000 cycles, as shown in Fig. 8. Although PPv nanospheres itself as a supercapacitor electrode suffers from a relatively poor cycling stability. The capacitance retention rate of PPy nanospheres is only 57.8% after 4000 cycles. However, the cycling stability of core-shell PPy-GO composite can be noticeably improved by modification with GO. The capacitance retention rate of PPy-GO reaches as high as 91.2% after 4000 cycles. To the best of our knowledge, the value is the highest ever reported for PPy-GO at such a smaller particle size of PPy nanospheres with only ~ 70 nm.[28] The improved cycling stability of PPv-GO can be attributed to the successive 3D network of the GO, as well as the well-defined core-shell nanostructures. It is worth mentioning that the synergistic effects from GO and PPy acts as an important role for the better stability of the core-shell PPy-GO nanocomposite, which would promote the mechanical strength of the composites during the charge/discharge process, as a result, avoided the disruption of electrode material.[41] Therefore, it is possible and viable that the core-shell nanospherical PPy-GO composite for 4000 cycles is very effective in the fabrication of safe and power-saving supercapacitors.

(Fig. 8 in here)

3.6.4 Electrochemical impedance spectroscopy

As a steady state technique with tiny potential variation, EIS is more dependable for testing the capacitance with minimized effect from non-capacitive Faradaic contributions, which can afford the ionic/electronic conductivity of the electrode materials during charging/discharging process.[42] Based on it, the electrodes of the core-shell nanospherical PPy-GO composites and PPy nanospheres were measured by EIS and the resulting Nyquist plots at open-circuit potentials are shown in Fig. 9. As can be seen, the Nyquist plot of the PPy-GO and PPy displayed a semicircle in the high frequency region and a straight line in the low frequency region. The internal resistance (Rs) is calculated from the high frequency intersection of the Nyquist plot in the x-axis, which is related to the internal resistance of the active material, ionic resistance of the electrolyte, and the contact resistance at the interface between active material and current collector. Meanwhile, the charge transfer resistance (Rct) is counted from the diameter of the single semicircle in the high frequency region. Usually, this resistance is associated with the diffusion of charge through the electrode/electrolyte interface.[43] It is observed that Rs of PPy and PPy-GO composite are 2.04 and 1.81 ohm, respectively. In addition, the Rct of PPy and PPy-GO composite are estimated to be 0.11 and 0.07 ohm, respectively. Obviously, the PPy-GO composite electrode displays lower Rs and Rct than PPy electrodes. Furthermore, the GO-PPy composite electrode represents a more perpendicular line than PPy electrodes at low frequency, implying better electrochemical capacitive behavior with fast ion diffusion. The EIS results are in good agreement with the observation from the CV and GCD tests results. Based on the discussion mentioned above, we could come to a conclusion that all these results also prove the positive synergistic effect between GO and PPy of the core-shell nanasphereical PPy-GO composite, and the electrochemical performance of the PPy-GO composite apparently were improved, which were favorable for electrode materical of supercapacitors.

(Fig. 9 in here)

4. Conclusions

In summary, the unique 3D core-shell nanospherical PPy-GO composites have been successfully fabricated by the facile method. This method provides an efficient approach to combine the pseudocapacitance of uniform PPy nanospheres with EDLCs of GO in 3D core-shell PPy-GO composites, which exhibit better electrochemical performance, good rate capability and excellent cycle stability with high mass loading due to the successive 3D core-shell structure and the strong interaction between PPy and GO substrate. Therefore, the unque 3D core-shell nanospherical PPy-GO composite is envisioned to be used as a promising electrode material and promotes their practical applications for electrochemical supercapacitors with improved performance.

Author Information

Corresponding Author

Fax: +86 (931) 8912113. E-mail: zhaogh@lzu.edu.cn, weih@lzu.edu.cn.

Acknowledgements

The authors would like to acknowledge the financial support provided by the National Natural Science Foundation of China (No. 21301081 and 21374045) and the Fundamental Research Funds for the Central Universities (Izujbky-2015-30).

References

- 1 P. Simon, Y. Gogotsi, Materials for electrochemical capacitors, *Nature materials*, 2008, 7, 845.
- 2 Q. Lu, J. G. Chen, Nanostructured Electrodes for High-Performance Pseudocapacitors, *Angewandte Chemie International Edition*, 2013, 52, 1882.
- 3 F. W. Richey, B. Dyatkin, Y. Gogotsi, Ion dynamics in porous carbon electrodes in supercapacitors using in situ infrared spectroelectrochemistry, *Journal of the American Chemical Society*, 2013, **135**, 12818.

Page 15 of 24

- 4 M. Winter, R. J. Brodd, What are batteries, fuel cells, and supercapacitors? *Chemical reviews*, 2004, **104**, 4245.
- 5 S. L. Candelaria, Y. Shao, W. Zhou, Nanostructured carbon for energy storage and conversion, *Nano Energy*, 2012, 1, 195.
- 6 L. Dong, Z. Chen, D. Yang, Hierarchically structured graphene-based supercapacitor electrodes, *Rsc Advances*, 2013, 3, 21183.
- 7 J. Cherusseri and K. K. Kamal, Self-standing carbon nanotube forest electrodes for flexible supercapacitors, *Rsc Advances*, 2015, **5**, 34335.
- 8 S. Li, D. Huang, J. Yang, Freestanding bacterial cellulose–polypyrrole nanofibres paper electrodes for advanced energy storage devices, *Nano Energy*, 2014, **9**, 309.
- 9 B. Wang, J. Qiu, H. Feng, Preparation of graphene oxide/polypyrrole/multi-walled carbon nanotube composite and its application in supercapacitors, *Electrochimica Acta*, 2015, **151**, 230.
- 10 S. Chabi, C. Peng, Z. Yang, Y. Xia, Y. Zhu, Three dimensional (3D) flexible graphene foam/polypyrrole composite: towards highly efficient supercapacitors, *Rsc Advances*, 2015, 5, 3999.
- 11 G. Ma, H. Peng, J. Mu, In situ intercalative polymerization of pyrrole in graphene analogue of MoS₂ as advanced electrode material in supercapacitor, *Journal of Power Sources*, 2013, **229**, 72.
- 12 J. H. Kim, S. H. Kang, K. Zhu, Ni-NiO core-shell inverse opal electrodes for supercapacitors, *Chemical Communications*, 2011, 47, 5214.
- 13 F. Shi, L. Li, X. L. Wang, Metal oxide/hydroxide based materials for supercapacitors, *Rsc Advances*, 2014, **4**, 41910.
- 14 W. Chen, R. B. Rakhi, H. N. Alshareef, Facile synthesis of polyaniline nanotubes using reactive oxide templates for high energy density pseudocapacitors, *Journal of Materials Chemistry A*, 2013, **1**, 3315.
- 15 R. Gangopadhyay, A. De, Conducting polymer nanocomposites: a brief overview, *Chemistry of materials*, 2000, **12**, 608.
- 16 X. Zhang, H. Zhang, C. Li, Recent advances in porous graphene materials for supercapacitor applications, Rsc Advances, 2014, 4, 45862.
- 17 L. Wei, G. Yushin, Nanostructured activated carbons from natural precursors for electrical double layer capacitors, *Nano Energy*, 2012, **1**, 552.
- 18 J. K. Gan, Y. S. Lim, A. Pandikumar, Graphene/polypyrrole-coated carbon nanofiber core-shell

- architecture electrode for electrochemical capacitors, Rsc Advances, 2015, 5, 12692.
- 19 S. Biswas, L. T. Drzal, Multilayered nanoarchitecture of graphene nanosheets and polypyrrole nanowires for high performance supercapacitor electrodes, *Chemistry of Materials*, 2010, **22**, 5667.
- 20 L. Z. Fan, Y. S. Hu, J. Maier, High electroactivity of polyaniline in supercapacitors by using a hierarchically porous carbon monolith as a support, *Advanced Functional Materials*, 2007, **17**, 3083.
- 21 D. R. Dreyer, S. Park, C. W. Bielawski, The chemistry of graphene oxide, *Chemical Society Reviews*, 2010, **39**, 228.
- 22 L. L. Zhang, S. Zhao, X. N. Tian, Layered graphene oxide nanostructures with sandwiched conducting polymers as supercapacitor electrodes, *Langmuir*, 2010, **26**, 17624.
- 23 F. Zhang, F. Xiao, Z. H. Dong, Synthesis of polypyrrole wrapped graphene hydrogels composites as supercapacitor electrodes, *Electrochimica Acta*, 2013, **114**, 125.
- 24 C. Zhu, J. Zhai, D. Wen, Graphene oxide/polypyrrole nanocomposites: one-step electrochemical doping, coating and synergistic effect for energy storage, *Journal of Materials Chemistry*, 2012, **22**, 6300.
- 25 L. Q. Fan, G. J. Liu, J. H. Wu, Asymmetric supercapacitor based on graphene oxide/polypyrrole composite and activated carbon electrodes, *Electrochimica Acta*, 2014, **137**, 26.
- 26 Y. Zhu, K. Shi, I. Zhitomirsky, Anionic dopant–dispersants for synthesis of polypyrrole coated carbon nanotubes and fabrication of supercapacitor electrodes with high active mass loading, *Journal of Materials Chemistry A*, 2014, **2**, 14666.
- 27 W. Wu, Y. Li, G. Zhao, Aldehyde–poly (ethylene glycol) modified graphene oxide/conducting polymers composite as high-performance electrochemical supercapacitors, *Journal of Materials Chemistry A*, 2014, 2, 18058.
- 28 T. Qian, S. Wu, J. Shen, Facilely prepared polypyrrole-reduced graphite oxide core–shell microspheres with high dispersibility for electrochemical detection of dopamine, *Chemical Communications*, 2013, **49**, 4610.
- 29 J. Yan, T. Wei, B. Shao, Preparation of a graphene nanosheet/polyaniline composite with high specific capacitance, *Carbon*, 2010, **48**, 487.
- 30 H. Wang, Q. Hao, X. Yang, Effect of graphene oxide on the properties of its composite with polyaniline, *ACS applied materials & interfaces*, 2010, **2**, 821.
- 31 D. Zhang, X. Zhang, Y. Chen, Enhanced capacitance and rate capability of graphene/polypyrrole

- composite as electrode material for supercapacitors, Journal of Power Sources, 2011, 196, 5990.
- 32 J. Zhang, X. S. Zhao, Conducting polymers directly coated on reduced graphene oxide sheets as high-performance supercapacitor electrodes, *The Journal of Physical Chemistry C*, 2012, **116**, 5420.
- 33 S. Bose, T. Kuila, M. E. Uddin, In-situ synthesis and characterization of electrically conductive polypyrrole/graphene nanocomposites, *Polymer*, 2010, **51**, 5921.
- 34 M. J. McAllister, J. L. Li, D. H. Adamson, Single sheet functionalized graphene by oxidation and thermal expansion of graphite, *Chemistry of Materials*, 2007, **19**, 4396.
- 35 S. Yang, C. Shen, Y. Liang, Graphene nanosheets-polypyrrole hybrid material as a highly active catalyst support for formic acid electro-oxidation, *Nanoscale*, 2011, **3**, 3277.
- 36 Z. Fan, J. Yan, T. Wei, Asymmetric supercapacitors based on graphene/MnO2 and activated carbon nanofiber electrodes with high power and energy density, *Advanced Functional Materials*, 2011, **21**, 2366.
- 37 A. S. Aricò, P. Bruce, B. Scrosati, Nanostructured materials for advanced energy conversion and storage devices, *Nature materials*, 2005, **4**, 366.
- 38 X. Lu, H. Dou, C. Yuan, Polypyrrole/carbon nanotube nanocomposite enhanced the electrochemical capacitance of flexible graphene film for supercapacitors, *Journal of Power Sources*, 2012, **197**, 319.
- 39 J. Mu, G. Ma, H. Peng, Facile fabrication of self-assembled polyaniline nanotubes doped with d-tartaric acid for high-performance supercapacitors, *Journal of Power Sources*, 2013, **242**, 797.
- 40 R. Kötz, M. Carlen, Principles and applications of electrochemical capacitors, *Electrochimica Acta*, 2000, **45**, 2483.
- 41 H. Zhou, G. Han, Y. Xiao, Facile preparation of polypyrrole/graphene oxide nanocomposites with large areal capacitance using electrochemical codeposition for supercapacitors, *Journal of Power Sources*, 2014, **263**, 259.
- 42 C. Peng, J. Jin, G. Z.Chen, A comparative study on electrochemical co-deposition and capacitance of composite films of conducting polymers and carbon nanotubes, *Electrochimica Acta*, 2007, **53**, 525.
- 43 X. Zhang, Y. Zhao, C. Xu, Surfactant dependent self-organization of Co₃O₄ nanowires on Ni foam for high performance supercapacitors: from nanowire microspheres to nanowire paddy fields, *Nanoscale*, 2014, **6**, 3638.

Figure captions

Figure 1 SEM (a,b) and TEM (c) images of PPy nanospheres; SEM (d,e) and TEM (f) images of the core-shell PPy-GO nanocomposites.

Figure 2 FT-IR spectra of GO, PPy nanospheres and the core-shell PPy-GO nanocomposites.

Figure 3 Raman spectra of GO, PPy nanospheres and the core-shell PPy-GO nanocomposites.

Figure 4 XRD patterns of GO, PPy nanospheres and the core-shell PPy-GO nanocomposites.

Figure 5 TGA curves of PPy nanospheres and the core-shell PPy-GO nanocomposites.

Figure 6 (a) CV curves of PPy and the core-shell PPy-GO electrodes at the scan rate of 100 mV/s, and (b) CV curves of the core-shell PPy-GO electrode at different scan rates of 10, 20, 40, 60, 80 and 100 mV/s in 1.0 M H₂SO₄ solution.

Figure 7 (a) GCD curves of PPy and the core-shell PPy-GO electrodes at the current density of 0.5 A/g, (b) GCD curves of the core-shell PPy-GO electrode at different current density of 0.5, 1.0 and 2.0 A/g in 1.0 M H₂SO₄.

Figure 8 Cycle stability of PPy and the core-shell PPy-GO electrodes during the long-term charge/discharge process.

Figure 9 Nyquist plots of PPy and the core-shell PPy-GO electrodes.

Scheme captions

Scheme 1 Illustration of the process for the preparation of PPy nanospheres.

Scheme 2 Proposed Possible Combinding Mode of PPy-GO Nanocomposites.

Table captions

Table 1 The polymerizing conditions in ice-water bath.

Table 2 The specific capacitance of the core-shell nanospherical PPy-GO composite and PPy nanospheres at different current densities in an aqueous 1.0 M H₂SO₄ electrolyte.

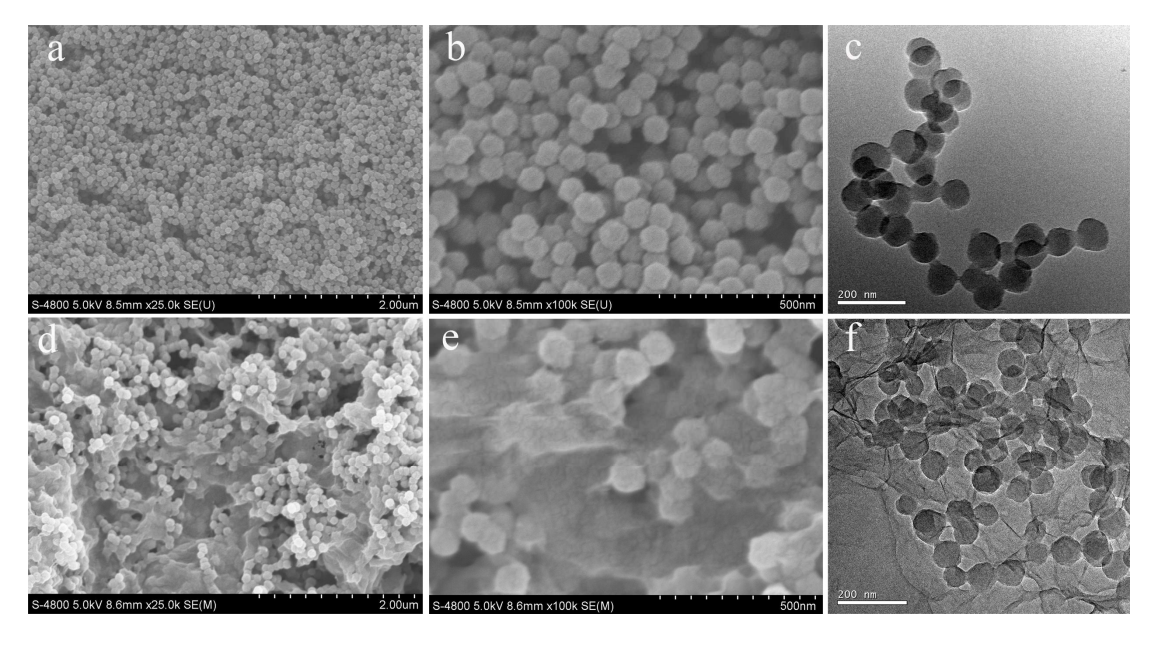


Figure 1 SEM (a,b) and TEM (c) images of PPy nanospheres; SEM (d,e) and TEM (f) images of the core-shell PPy-GO nanocomposites.

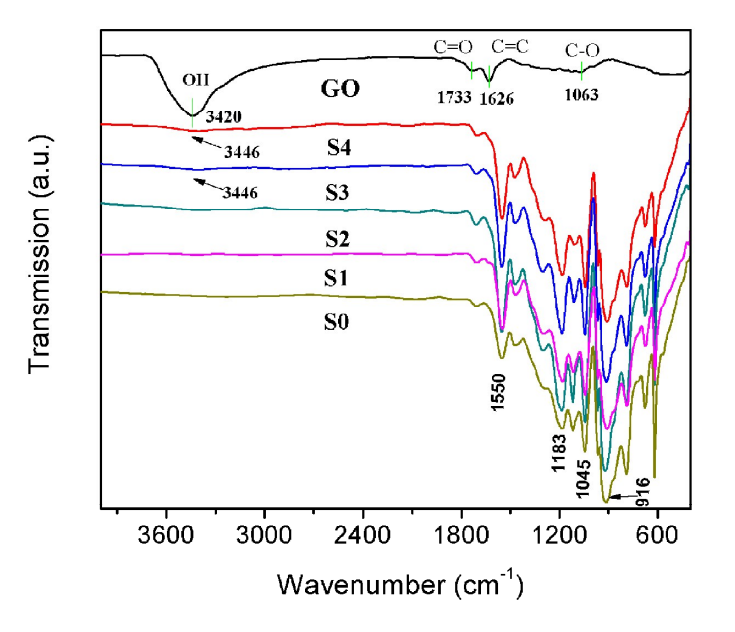


Figure 2 FT-IR spectra of GO, PPy nanospheres and the core-shell PPy-GO nanocomposites.

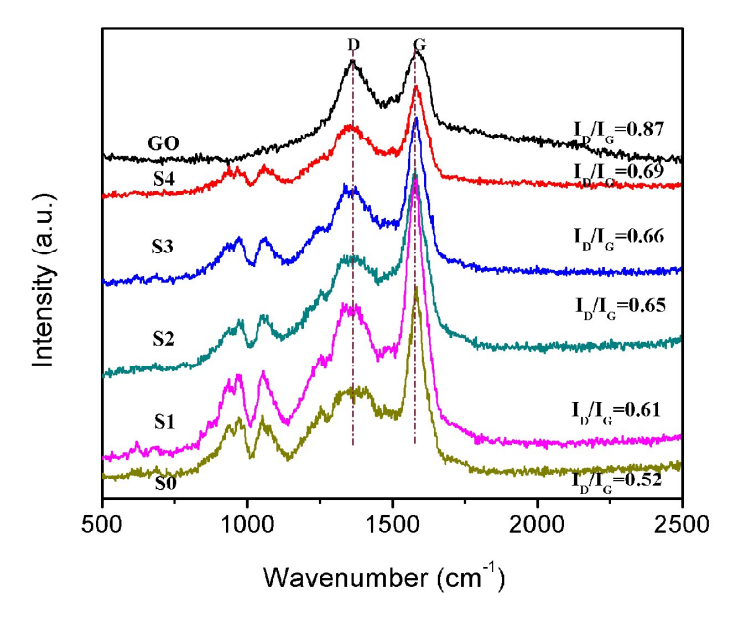


Figure 3 Raman spectra of GO, PPy nanospheres and the core-shell PPy-GO nanocomposites.

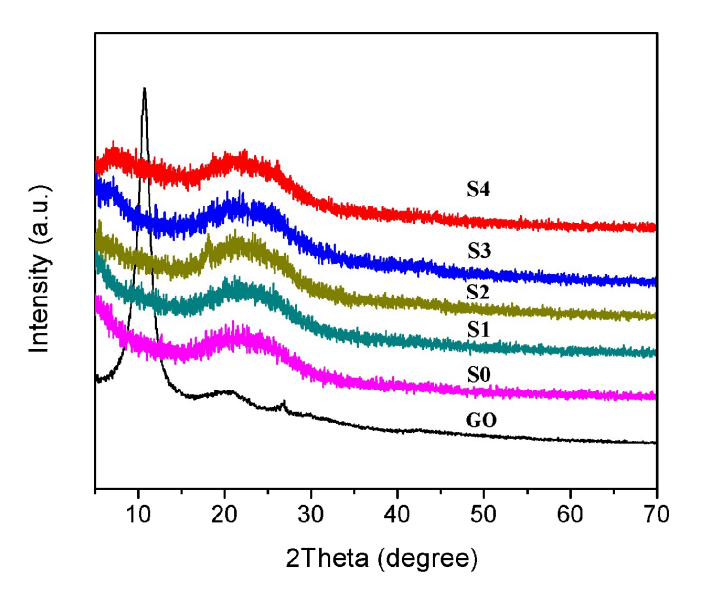


Figure 4 XRD patterns of GO, PPy nanospheres and the core-shell PPy-GO nanocomposites.

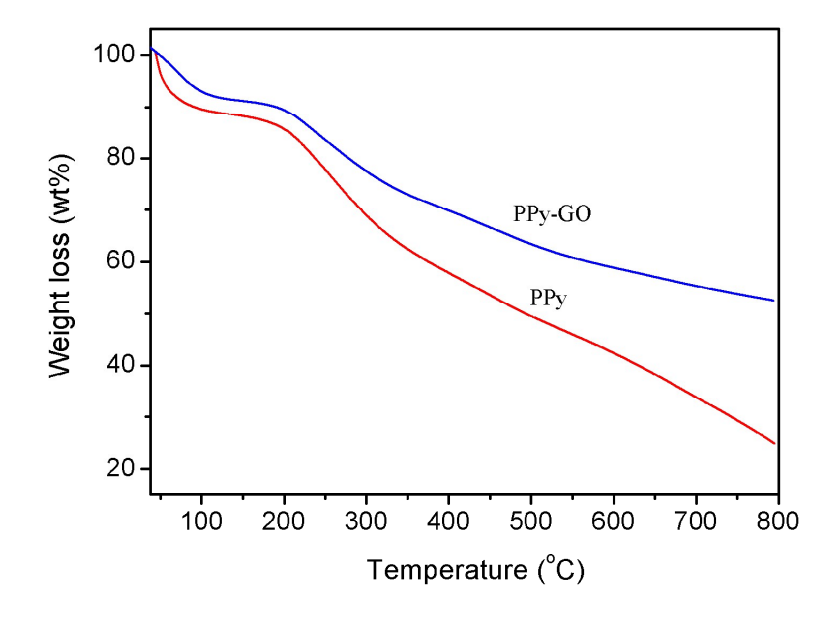


Figure 5 TGA curves of PPy nanospheres and the core-shell PPy-GO nanocomposites.

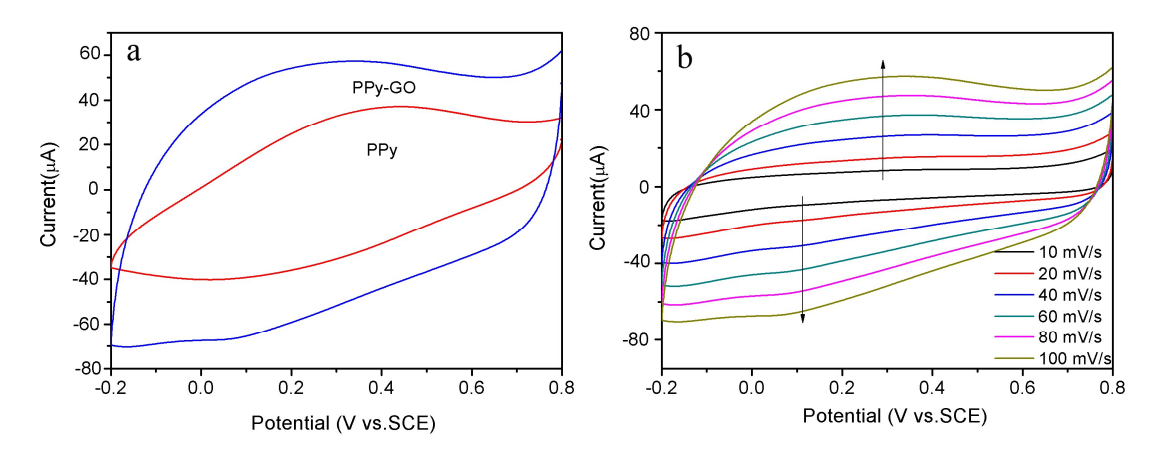


Figure 6 (a) CV curves of PPy and the core-shell PPy-GO electrodes at the scan rate of 100 mV/s, and (b) CV curves of the core-shell PPy-GO electrode at different scan rates of 10, 20, 40, 60, 80 and 100 mV/s in 1.0 M H₂SO₄ solution.

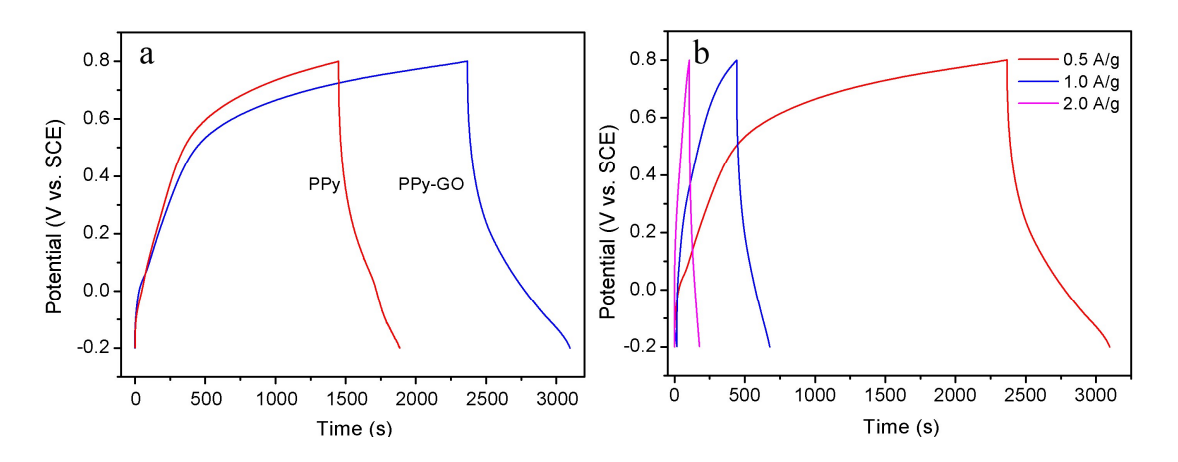


Figure 7 (a) GCD curves of PPy and the core-shell PPy-GO electrodes at the current density of 0.5 A/g, (b) GCD curves of the core-shell PPy-GO electrode at different current density of 0.5, 1.0 and 2.0 A/g in 1.0 M H₂SO₄.

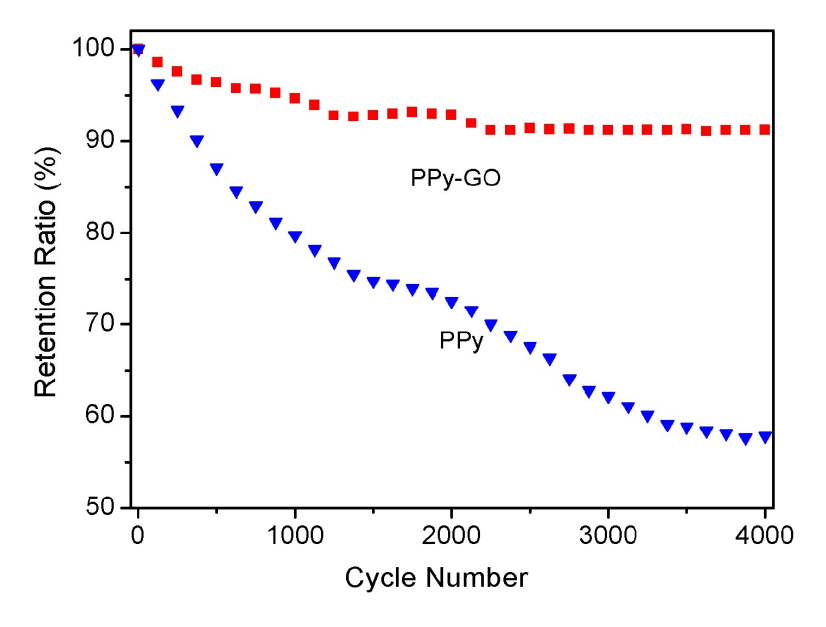


Figure 8 Cycle stability of PPy and the core-shell PPy-GO electrodes during the long-term charge/discharge process.

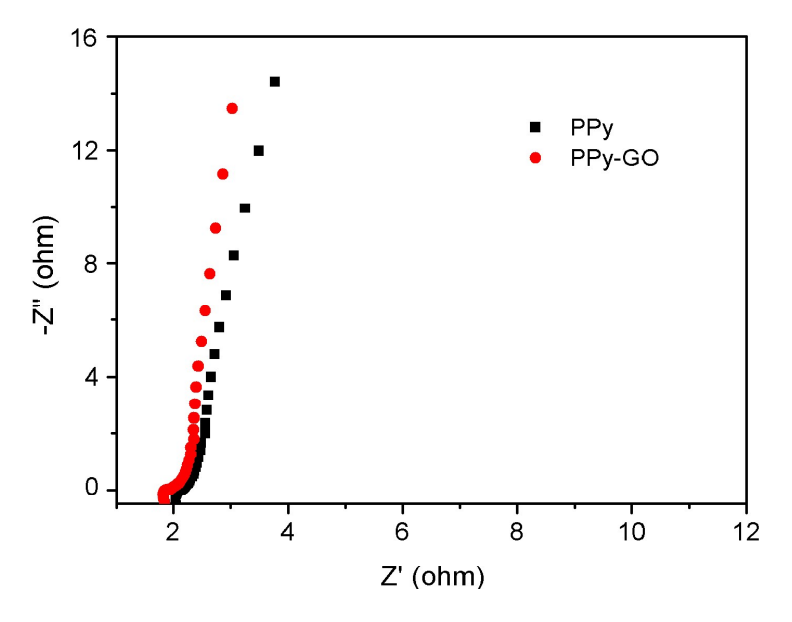
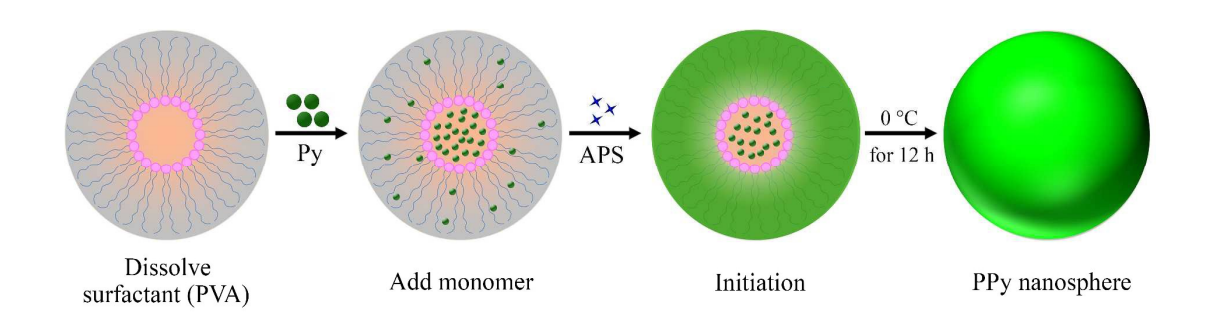


Figure 9 Nyquist plots of PPy and the core-shell PPy-GO electrodes.



Scheme 1 Illustration of the process for the preparation of PPy nanospheres.

Scheme 2 Proposed Possible Combinding Mode of PPy-GO Nanocomposites.

Table 1 The polymerizing conditions in ice-water bath.

PPy-GO samples	Py (mL)	GO (mL)	APS (g)
S0	0.5	0	1.14
S1	0.5	15 (3.5 mg/mL)	1.14
S2	0.5	30 (3.5 mg/mL)	1.14
S3	0.5	45 (3.5 mg/mL)	1.14
S4	0.5	60 (3.5 mg/mL)	1.14

Table 2 The specific capacitance of the core-shell nanospherical PPy-GO composite and PPy nanospheres at different current densities in an aqueous 1.0 M H₂SO₄ electrolyte.

Samples	Specific capacitance (F/g)		
	0.5 A/g	1.0 A/g	2.0 A/g
PPy-GO	370	233	144
PPy	216	143	68